SAND2000-0159J

The onset of pileup in nanometer-scale contacts

K.F. Jarausch, North Carolina State University, Raleigh NC.
J.D. Kiely, Sandia National Laboratories, Albuquerque NM.
J.E. Houston, Sandia National Laboratories, Albuquerque NM.
P.E. Russell, North Carolina State University, Raleigh NC

DISCLAIMER

ABSTRACT

The interfacial force microscope (IFM) was used to indent and image defect free Au (111) surfaces, providing atomic-scale observations of the onset of pileup and the excursion of material above the initial surface plane. Images and load-displacement measurements demonstrate that elastic accommodation of an indenter is followed by two stages of plasticity. The initial stage is identified by slight deviations of the load-displacement relationship from the predicted elastic response. Images acquired after indentations showing only this first stage indicate that these slight load relaxation events result in residual indentations 0.5 to 4 nm deep with no evidence of pileup or surface orientation dependence. The second stage of plasticity is marked by a series of dramatic load relaxation events and residual indentations tens of nanometers deep. Images acquired following this second stage document 0.25 nm pileup terraces which reflect the crystallography of the surface as well as the indenter geometry. Attempts to plastically displace the indenter 4-10 nanometers deep into the Au (111) surface were unsuccessful, demonstrating that the transition from stage I to stage II plasticity is associated with overcoming some sort of barrier. Stage I is consistent with previously reported models of dislocation nucleation. The dramatic load relaxations of stage II plasticity, and the pileup of material above the surface, require cross-slip and appear to reflect a dynamic process leading to dislocation intersection with the surface. The IFM measurements reported here offer new insights into the mechanisms underlying the very early stages of plasticity and the formation of pileup.

INTRODUCTION

The deformation characteristics of nanometer-scale contacts are of fundamental importance for processes ranging from tribology to precision machining. Nanoindentation has become a widely used technique for measuring the mechanical properties of such contacts. Much of the work has focused on identifying the onset of plasticity and describing the subsequent plastic evolution of such contacts (for recent reviews see [1] for metals and [2] for ceramics). Yield strengths comparable to the predicted ideal strength of the lattice have been measured in indentations of defect free single crystal Au surfaces [3-7]. Until recently most authors concluded that the onset of plasticity is signaled by the first dramatic relaxation in the load-displacement relationship during indentation [3,5,6,10]. In load controlled nanoindentation instruments such relaxation events are identified by sudden displacement excursions and have therefore been referred to as a 'pop-in' events [1-2,6-13]. For displacement controlled nanoindenters such relaxations are identified by sudden drops in load [3-5]. For the purposes of this paper dramatic relaxations (characterized by more than a 5% drop in load for displacement controlled instruments) will be referred to as 'major' events.

Recent reports have shown that plasticity can occur prior to the first major event [1,4,8,9,11-13]. These reports suggest that the initial stage of plasticity is identified by slight relaxations in the load-displacement relationship. These subtle relaxations will be referred to as 'minor' events (less than a 5% drop in load for displacement control) for the purposes of this investigation. Kiely et al. showed that both minor and major events occur during the deformation of Au (111) surfaces [4]. The yielding behavior of Fe-3 wt.% Si also suggests that plasticity can occur at much lower loads than that required for the first major event [1,8,9,11-13]. Despite the extensive study of nanometer scale contacts, the nature of plastic relaxation events and the mechanisms underlying pileup formation are still not well understood. In this report we show that major events are always associated with the formation of pileup, the excursion of material above the initial surface plane.

Structural investigations of the deformation of nanometer scale contacts have been supported by a variety of microscopy techniques [1,9,10,13,14] and molecular dynamics simulations [15-19]. Transmission electron microscopy (TEM) studies have been limited to indentations greater than 50 nanometers in depth from which large numbers of dislocations have been generated (obscuring the initial stages of plasticity) [1,9,10,13]. Scanning probe microscope (SPM) techniques have been used to investigate the surface structure after indentation [1,4-7,9,10,13,16] to identify the extent of the plastic zone. Isolated dislocation structures, associated with the deformation of a Au (100) surface, have been observed with a STM [20]. To date most models describing plastic evolution of

contacts have been constructed from observations of the activated slip systems and the dislocation density as a function of distance from the indentation [1,9,10,13]. Molecular dynamics simulations are now being used in an effort to understand the deformation mechanisms in more detail [15-19]. These simulations have suggested that the elastic accommodation of an indenter is followed by an initial stage of plasticity which differs from the latter stages of dislocation generation and propagation [18,19]. Size limitations prevents these simulations from extending into the later stages of plasticity and studying pileup formation. At present no direct observations of the structural evolution of a contact from the initial nucleation event to the latter stages of multiplication and cross-slip have been reported. As a result, the mechanisms which underlie the formation and evolution of pileup around an indentation are still not well understood.

In this paper, an interfacial force microscope (IFM) was used to indent a parabolic and a three-sided diamond into Au (111) surfaces to measure the dependence of plasticity on defect type. Since the IFM operates under displacement control and its load sensor is feedback controlled, the indenter is not pushed further into the material after the onset of a load relaxation event. This allows the IFM to resolve the magnitude of the load relaxations as well as the structure of the contact immediately after such events. The imaging resolution of the IFM provides atomic scale information about the surface structure after indentation. Images acquired before and after indentation and the load-displacement curves obtained during indentation were used to investigate the structural evolution of nanometer-scale contacts. The onset of plasticity and the formation of pileup are discussed in the context of dislocation mechanics.

THE EXPERIMENT

All indentations were performed with an IFM on Au (111) surfaces at room temperature. The IFM, described in detail elsewhere [21], combines the imaging capability of a SPM with a stable feedback controlled load sensor for quantitative force-displacement measurements. Gold single crystals with (111) surface orientations were prepared by flame annealing high purity (99.99%) Au wires to form faceted balls [5]. After preparation the surfaces have very low defect densities and are characterized by wide terraces (>250 nm) separated by individual and multiple steps [5,6]. Immediately after annealing the samples were immersed in a 0.5 mM solution of hexadecanethiol [$CH_3(CH_2)_{15}SH$] to allow the self-assembly of a monolayer. The alkane-thiol monolayer has been shown to passivate the chemical and adhesive interactions between an indenter and the Au [22]. Measurements were performed in a drop of hexadecane to minimize Van der Waals interactions between the indenter and the Au.

Load-displacement measurements were obtained by displacing the diamond indenters into Au (111) surfaces at a constant rate (10 nm/s) while recording the force acting on the indenter. The Hertzian contact model was used to determine the elastic modulus and shear stress value at yield from the load-displacement curves [23,24]. For the purposes of this investigation 'pileup' is defined as any material, that after indentation, remains displaced above the initial surface. 'Residual indentation' describes the volume of material that remains displaced below the initial surface after indentation. The depths of the residual indentations were measured from the hysteresis of the load-displacement curves acquired during indentation (equal to the displacement difference between the initial contact and the final unloading points). The IFM was used to acquire images before and after the indentations using constant force feedback at loads of less than 100 nN. Repeated scans of the same areas at these loads did not result in damage to the Au (111) surfaces. All images were acquired using the same diamonds with which the indentations were performed. The resulting image convolution obscures the depth and sub-surface geometry of the residual indentations, but still allows for surprisingly good resolution of the surface features and pileup surrounding the indentations.

The IFM was equipped with a three-sided and a parabolic diamond indenter whose geometries were shaped using a focused ion beam micromachining process [25]. Indentations were performed with these two different geometries to study the effects of indenter imposed stress concentration on the formation of pileup. A 'three-sided' diamond was prepared with a Berkovitch geometry extending to within 20 nm of the diamond's apex (Fig. 1(a)-(c)). The apex was roughly parabolic and characterized by a 50 nm radius of curvature. A 'parabolic' diamond was prepared with a smooth parabolic geometry extending from 500 nm all the way to the diamond's apex (Fig. 1(d),(e)). This indenter was characterized by a 100 nm radius of curvature. The diamond indenter geometries were determined by imaging in-situ probe characterizing structures [26] and independently verified using a scanning electron microscope [27]. The geometry of these indenters determines the stress distribution applied to the Au (111) surfaces during indentation [23,24]. The smaller end-radius and the eventual influence of the edges (for indentations deeper than 20 nm) of the three-sided diamond results in higher stress concentrations during indentation than for the parabolic indenter. This difference affects the yield threshold(s) as well as the subsequent evolution of pileup.

THE TWO STAGES OF PLASTICITY

A load-displacement curve illustrating the elastic response of a Au (111) surface is shown in Fig. 2. The force acting on the three-sided diamond indenter is plotted as a

function of the relative displacement of the surface and the indenter. The lack of hysteresis between the loading and unloading curves is the signature of an elastic contact. Images acquired before and after the indentation confirm that the indentation did not cause any residual indentation (to within 0.1 nm). An elastic modulus of $E^* = 68 \pm 2$ GPa was determined from the Hertzian fit (shown by the dashed line) of the load-displacement data. This value is quite close to literature values of 70 GPa for bulk gold. The elastic response shown in Fig. 2 is characteristic of measurements with the parabolic and three-sided diamonds for indentation depths of less than 8 nm and 5 nm respectively (for which the stresses applied during indentation do not exceed 1 GPa). It is worth noting that the presence of the alkane-thiol monolayer aids the formation of an elastic contact by passivating the adhesive (chemical) interactions between the indenter and the surface [22].

A load-displacement curve measured during an indentation, which resulted in a residual indentation 0.5 nm deep, is shown in Fig. 3(a). This measurement was obtained by displacing the three-sided indenter 12 nm into a Au (111) surface. The onset of plasticity at approximately 7 μN is identified by the point at which the load response deviates from the Hertzian fit (marked by an arrow). This event is characterized by a slight relaxation in the load with respect to the Hertzian prediction. After this first minor event the force continues to rise at the rate shown by the solid line, nearly parallel to the Hertzian fit (dashed line) but with an offset in displacement. This suggests that the initial plastic event is followed by elastic response, with an offset from the Hertzian prediction equal to the magnitude of the plastic deformation. However recent calculations have shown that although the force appears to continue rising in a Hertzian manner, the contact may be responding in an elastic-plastic fashion [8]. Figure 3(a) shows that as the load rises further (above 20 μN) it increases at a lesser rate than predicted by the Hertzian fit indicating that the response is not purely elastic. This suggests that the first plastic event is followed by elastic-plastic behavior which will subsequently be referred to as stage I plasticity. The onset of stage I plasticity is marked by the first minor event, the first deviation from the elastic (Hertzian) prediction. Subsequent stage I plasticity is characterized by an elastic-plastic response and results in residual indentations ranging from 0.5 to 4 nm. In some cases discrete relaxation (minor) events are apparent throughout stage I plasticity while in other measurements the load appears to increase smoothly. These subtle relaxation events are near the current detection limits of the IFM load sensor and so their presence in the 'smooth' curves cannot be ruled out. Stage I plasticity was observed when displacing the parabolic indenter from 8 to 20 nm into the surface while for the three-sided diamond, from 5 to 12 nm into the surface.

Images acquired before and after an indentation showing only stage I plasticity are shown in Fig. 3(b) and (c). The residual indentation appears round and shows no correlation with the crystallography of the Au (111) surface. The cross-section shown in Fig. 3(d) indicates that the residual indentation is 0.5 nm deep which confirms the plasticity evident the load-displacement curve (Fig. 3(a)). The roughly circular shape of deformation shown in Fig. 3(c) is a typical result of indentations showing only stage I plasticity. This suggests that the geometry of residual indentations, due only to stage I plasticity, is governed by the shape of the indenter and not by the crystallographic orientation of the surface. IFM images show no evidence of pileup (less than 0.1 nm deviation from the initial surface plane) near such residual indentations. Repeated scans of the same indentation sites showed no evidence of these residual indentations changing or healing as a function of time.

The load-displacement curve of an indentation which resulted in the formation of pileup is shown in Fig. 4. Three types of deformation are evident in this load-displacement curve. Initially the Au (111) surface accommodates the indenter elastically and the load response matches the Hertzian prediction (shown by the dashed line). At a load of approximately 7 μN the load-response begins to deviate from the elastic (Hertzian) prediction signaling the onset of stage I plasticity. The load continues to increase as the Au (111) surface deforms further (stage I plasticity) until a load of approximately 40 μN is reached. At this point the force acting on the indenter suddenly drops to zero, before increasing again as the indenter is displaced further into the material. Such a dramatic relaxation reflects a change in the yielding behavior of the contact and will subsequently be referred to as the onset of stage II plasticity. These kinds of major relaxation events have been reported in nanoindentation measurements of a variety of defect-free surfaces [1-13]. The dramatic drop in load shown in Fig. 4 would appear as a sudden step-in or 'pop-in' displacement excursion for load controlled instruments [1,2,7-13]. Unlike in most of these reports, we found that the displacement and force values associated with this first major event were highly repeatable for indentations into Au (111) regions free of surface steps and other defects (within ±2 nm, and ±5 μN respectively). The onset of stage II plasticity is signaled by this first major event or load relaxation. As the indenter is displaced further into the material the force increases again, at first elastically and then plastically, until another, albeit less dramatic, load-relaxation event occurs (Fig. 4). The repetition of this loading-unloading cycle is characteristic of stage II plasticity [4]. Stage II was observed when displacing the parabolic indenter more than 20 nm into the surface. Stage II was observed when displacing the three-sided diamond more than 12 nm into the surface.

Indentations were performed with both the three-sided and the parabolic indenter for a continuous range of displacements into the surface (from 2 to 100 nm). The hysteresis of the load-displacement curves acquired during indentation was used to measure the depth of the residual indentations. From this analysis it was determined that indentations showing only stage I plasticity resulted in depths ranging from 0.5 to 4 nm for the three-sided indenter and from 0.5 to 8 nm for the parabolic indenter. Indentations showing both stage I and stage II plasticity resulted in depths exceeding 11 nm for the three-sided indenter and exceeding 20 nm for the parabolic indenter. No residual indentations with depths from 5 to 10 nm, for the three-sided indenter, and from 10 to 20 nm deep, for the parabolic indenter, were recorded. These observations suggest that the transition from stage I to stage II plasticity is associated with overcoming some sort of plasticity barrier.

THE FORMATION OF PILEUP

IFM images acquired after indenting reveal that stage II plasticity is always associated with the formation of pileup. Images acquired after withdrawing the indenter immediately after the first major event show clear evidence of pileup. Figures 5 and 6 are representative of the images obtained after indentations showing both stage I and II plasticity. The image shown in Fig. 5 was obtained after displacing the three-sided indenter 27 nm into an Au (111) surface. The image shown in Fig. 6 was obtained after displacing the parabolic indenter 50 nm into the same surface. The geometry of the pileup shown in these images reflects the crystallographic orientation of the Au (111) surface as well as the stress concentration imposed by the indenters.

The formation of pileup for the three-sided indenter is controlled by both the orientation of the gold surface and by the geometry of the indenter (Fig. 5). The load-displacement relationship measured during this indentation showed both stage I and stage II plasticity (Fig. 4). The pileup regions are visible as terraces which are raised 0.25 nm above the initial surface and extend radially outward from the indentation site (Fig. 5). They can extend out as much as 500 nm from the indentation site and are bounded by edges which display the same trigonal symmetry as the steps found on the pre-indentation Au (111) surface. From this observation we conclude that these terraces are bounded by the intersection of sub-surface (111) planes and the Au (111) surface. Such a geometry is consistent with the deformation of FCC metals which is known to occur on the 12 octahedral slip systems {111}<110>. The residual indentation also has a triangular shape but it is not perfectly aligned with the crystallographic orientation of the Au (111) surface. This suggests that the shape of the three-sided indenter controls the geometry of the

residual indentation while the crystallography of the gold (and the associated dislocation mechanisms) controls the pileup formation. From similar images it is apparent that two lobes of pileup, visible as terrace bunches, extend outward from each face of the indenter while terrace formation does not occur at the indentation corners. This pattern suggests a preference for pileup formation as a six-fold rosette which is distorted by the stress concentration imposed by the indenter faces. Pileup formation is driven by the compressive stresses at the indenter faces, and suppressed by the tensile stresses at the indenter corners. Based on a series of indentations, we report that the number of terraces contained in each lobe increases with increasing indentation depth, eventually forming the rounded hillocks commonly reported as pileup in the literature [1,9-11,28].

Figure 5 demonstrates how the formation of pileup is effected by the proximity to prior indentations. A prior indentation was performed 1.2 μm from the indentation shown in the center of Fig. 5. Pileup terraces extending from this prior indentation are visible in the upper right corner of the image (Fig. 5). The close proximity of these two indentations suppressed the formation of pileup from the face of the indenter whose surface normal was directed towards the previous indentation.

The formation of pileup for the axi-symmetric parabolic indenter is dominated by the crystallography of the surface (Fig. 6). The image appears less clear than Fig. 5 because the broader radius of the parabolic diamond reduces the imaging resolution of the IFM. The load-displacement relationship measured during this indentation showed both stage I and stage II plasticity. The residual indentation shows three-fold symmetry (aligned with the surface steps) which indicates that the (111) slip systems, and not the geometry of the indenter, control the deformation geometry. This result is not surprising since the stresses imposed by the indenter are distributed uniformly during indentation. Residual indentations with three-fold symmetry, on (111) surfaces, were previously reported by Kiely et al. [5]. The pileup regions are visible as lobe shaped terraces which are raised 0.5 to 2 nm above the initial surface and extend outward from the indentation site about 500 nm. Six of these lobe-terraces are distributed around the indentation site forming a rosette pattern (Fig. 6). Each of the three deformation faces is associated with two lobes of pileup in a manner similar to that observed for the three-sided indenter. The slight asymmetry of the rosette is most likely due to a misalignment of the indentation axis and the surface normal. The precise edge geometries and heights of these lobes are difficult to determine since the parabolic indenter does not image the surface with the resolution provided by the three-sided indenter. A series of indentations ranging from 30 to 60 nm into the surface confirms that the height of these lobe shaped terraces increases with increasing indentation depth.

DISCUSSION

The load-displacement measurements and images reported here suggest that pileup is the result of a dynamic energy-conversion process which occurs after a barrier to further plasticity is overcome. Images show that the transition from stage I to stage II plasticity is always associated with the formation of pileup. Load-displacement measurements show that the first major load relaxation event is the signature of a sudden conversion of the elastic strain energy stored in the material surrounding the material neighboring the contact (responsible for the load on the indenter). Most of the elastic strain energy is lost to internal friction during the formation and propagation of dislocation structures. A smaller fraction of the strain energy remains stored in the deformation structures surrounding the contact (and does not load the indenter). The slope of the load-displacement relationship during one of these major relaxations is governed by the time constant of the IFM load sensor indicating that this conversion process takes place in less than 1 msec (the sensor's time constant). Measurements of indenter displacement indicate changes of less than 0.01 nm during these relaxations. In the following, these results are discussed in the context of previous studies of indentation plasticity.

Previous experimental studies of the evolution of plasticity can been grouped into two categories as suggested by Bahr et al. [1]. Some authors have concluded that the first major, or 'pop-in', event reflects the nucleation of dislocations [3,5,6,10] while others have suggested the possibility of dislocation activity prior to this event [1,4,8,9,11-13]. Our IFM images and load-displacement curves show clear evidence that plasticity can occur prior to the first major relaxation event. The atomic-scale deformations of stage I plasticity reported here are near or below the load and image resolution limits of current nanoindentation measurements [1-9]. Therefore, their presence in previous work cannot be discounted, as has been suggested [1,2,7-13]. Several authors have proposed that plasticity prior to major events reflects the nucleation and propagation of a very small number of dislocations (less than 100) which are 'geometrically necessary' to accommodate the indenter [7-9,12,13]. They suggested that this nucleation and propagation process proceeds until the backforces are sufficient to arrest the penetration of the indenter (for load-controlled measurements) [7-9,12,13]. This latter theory is not readily applied to displacement controlled measurements. These authors propose that the next stage of plasticity, whose onset is signaled by a major event, requires the activation of dislocations on additional slip systems [7-9,12,13]. IFM images acquired after indentations showing only stage I behavior appear to reflect the geometry of the indenter (within the imaging resolution) and therefore support the notion that the first dislocations are geometrically

necessary. The subtle elastic-plastic behavior recorded in the load-displacement curves during stage I plasticity is also consistent with the nucleation and propagation of a small number (less than 100) of dislocations.

The precise evolution of plasticity and the subsequent formation of pileup is critically dependent on the geometry of the very first dislocations which are nucleated under the contact. In the pioneering work of Kelchner et al. [15], molecular dynamics simulations were used to study the nucleation of dislocations during indentation of a Au (111) surface. Their work showed that partial dislocation loops are nucleated beneath the surface on (111) planes at about half of the total indentation depth and near the edges of the contact [15]. The nucleation events are associated with slight relaxations in the load-displacement relationship, very similar to those reported here as stage I plasticity. Their simulations show that these first dislocation loops expand downward towards the center of the contact as the indenter is displaced further into the material. Eventually the dislocation structures meet underneath the indenter and become entangled. This prevents further propagation on the slip systems activated by the initial nucleation events. The continued elastic and plastic evolution of the contact therefore requires the activation of additional slip systems. By cross-slipping these first dislocations could change their direction of propagation and be attracted, by the image force, to the free surface eventually forming pileup. Due to current computational limitations these simulations have not yet extended past the initial nucleation and propagation stage of plasticity. As a result, the processes associated with dislocation entanglement and cross-slip, and therefore the precise nature of major relaxation events, remains unclear.

Bahr et al. concluded that for Fe 3 wt.% Si, the first major relaxation event is tied to oxide breakthrough which allows dislocation emission at the surface and results in pileup formation [8,12,13]. Subsequent studies of yielding phenomena as a function of oxide thickness have shown that this explanation is not sufficient [1]. Our measurements were performed on the oxide-free surface of Au (111) and we propose instead that the first major event is a result of overcoming a barrier to cross-slip and reflects the subsequent dynamic release of the elastic energy stored in this contact. The consistency of the IFM load-displacement measurements suggest that the dynamic relaxation process is triggered by overcoming a distinct barrier (at indentation depths of 12±2 nm for the three-sided indenter). Based on our measurements we find that immediately prior to this first major event, elastic stresses on the order of 8 GPa are present in the contact [23,24]. We propose that once the barrier for cross-slip is overcome, the dislocations generated during stage I plasticity are free to propagate again which requires much less strain energy than cross-slip. The tremendous elastic energy stored in the contact can therefore be quickly released. In

effect, a wave of strain energy is released once the barrier to cross-slip is overcome. This wave of strain energy radiates outward from under the indenter until it has dissipated enough for the indenter and the surface to reach a new static equilibrium. We propose that it is this release which results in the formation of the pileup around the indentation. This conclusion is supported by IFM images which show pileup after indentations where the indenter was withdrawn immediately after the first major event occurred.

Images acquired after indentation confirm that the transition from stage I to stage II plasticity is associated with overcoming a barrier to further plasticity. IFM images show that the elastic-plastic response of stage I plasticity does not result in the formation of pileup although it causes residual indentations 0.4 to 4 nm deep for indentations with the three-sided indenter (0.4 to 8 nm for the parabolic indenter). In contrast, the major load relaxations associated with stage II plasticity always cause the formation of pileup while resulting in residual indentations exceeding 10 nm (20 nm for the parabolic indenter). No residual indentations from 4 to 10 nm deep were observed (from 8 to 20 nm for the parabolic indenter). This gap in the recorded plastic displacements demonstrates that the first major event reflects an avalanche of plasticity, resulting in much deeper residual indentations and the formation of pileup.

IFM measurements performed near (within 0.5 μm) prior indentations or other defects (surface steps, slip bands) demonstrate that the evolution of plasticity and the formation of pileup is effected by the presence of such defects. Previous IFM measurements reveal that the first major event occurs for lower values of applied stress in the presence of defects [6]. This result suggests that the stress concentration and strain energy associated with the defects may effect the barrier for cross-slip during an indentation. The presence of defect structures also effects the magnitude of the major relaxation events. When indenting near surface steps, or previous indentations, the relaxations are arrested at load drops ranging from 25 to 75% of the load prior to the event instead of proceeding to a 100% drop as they do in defect free regions. The arrest of the major load relaxations in the presence of defects demonstrates that these defects limit the conversion of elastic energy to plastic energy, perhaps by partially preventing the propagation of dislocations. This conclusion is substantiated by the screening of pileup due to a prior indentation as shown in Fig. 6. The effects of defect structures on stage II plasticity and the formation of pileup can be summarized by considering the strain energy stored and then released in the contact during indentation. The threshold for, and magnitude of, a major event is a function of the energy that is stored in the material surrounding the indenter at the initiation of the event. The energy required for such an

event, and then released by the event, is reduced by the presence of prior defect structures which are associated with a stored strain energy.

The geometry of the pileup regions reflects how the favored slip systems respond to the stress concentration imposed by the indenters. The geometry of the pileup terraces suggests that the wave of strain energy which is released by a major event propagates on the most favored slip systems. The precise geometry of this strain wave appears to be governed by the stress concentrations imposed by the geometry of the indenter. The asymmetric stress distribution imposed by the three-sided indenter results in an irregular pattern of pileup terraces for each indenter face. This is consistent with the misalignment of the three-sided indenter with respect to the Au lattice. The asymmetric stress distribution imposed by the indenter favors some slip systems over others. In contrast, the symmetric stress distribution imposed by the parabolic indenter results in an evenly distributed six-fold rosette pattern, since the favored slip systems respond equally. Rosette patterns resulting from indentation of Ag (111) surfaces have been observed using etch staining techniques [14].

The IFM images suggest that pileup formation is the direct consequence of dislocation emission. The measured 0.25 nm step heights of the pileup terraces agree remarkably well with spacing of the (111) planes coplanar with the surface. This 0.25 nm step height was measured as the average step height on the freshly prepared Au (111) surface. This suggests that pileup formation is the result of a block of material being displaced upwards by single, or multiple lattice steps. A more rigorous description of the dislocation structure responsible for the observed pileup terraces is beyond the scope of this report and will likely require large scale molecular dynamics simulations.

The model of pileup formation described here is proposed as the most likely explanation of our IFM based observations but several additional factors cannot be ruled out. The contribution of creep (especially surface diffusion) to the early stages of plasticity has been reported [29,30]. Given the high surface diffusivity of gold at room temperature this mechanism could contribute to our observations of stage I plasticity. If stage I plasticity is entirely due to creep, then the first major event must reflect the nucleation of dislocations under the indenter. Given the likely structure of the first dislocation loops [15] however, it is unlikely that they, during the subsequent load relaxation, would be able to propagate towards the surface without first cross-slipping. Furthermore, calculations suggest that creep is too slow to account for the penetration rates common in nanoindentation [29] and therefore cannot entirely account for stage I plasticity. A contribution of the IFM load sensor to the load relaxation measured during a major event cannot be ruled out. The plasticity cascade of a major event reflects dislocation propagation

and is therefore expected to happen on a sub micro-second time scale while the force feedback only responds with a milli-second time constant. It is therefore possible that the load sensor contributes to the plastic relaxation during a major event by pushing the indenter further into contact. Our measurements of the load sensor show that the indenter moves less than 0.01 nm during such an event and we therefore expect this contribution to be slight. Although the contribution of creep and instrument response cannot be ruled out, we expect that these factors do not significantly effect our observations.

CONCLUSIONS

Atomic scale images documenting the onset of pileup in nanometer-scale contacts have been reported. The IFM images and load-displacement measurements show that the elastic accommodation of the indenter is followed by two stages of plasticity. The first stage results in atomic scale residual indentations and is not associated with the formation of pileup. The onset of the second stage of plasticity is signaled by the first major load relaxation event. This first major event and subsequent stage II plasticity are always associated with the formation of pileup. IFM images demonstrate that the onset of pileup is characterized by terraces raised in multiples of 0.25 nm above the initial surface and bounded by (111) planes. The images show a distribution of two lobes of pileup terraces per indenter face, forming a six-fold rosette pattern around the indentation. Analysis of the load-displacement curves and images suggest that the first major load relaxation event is associated with overcoming a barrier to cross-slip. Once this barrier has been overcome, a dynamic avalanche of plasticity occurs and it is this relaxation process which results in the formation of pileup. The results reported here offer new insight into the early stages of plasticity and the formation of pileup in nanometer scale contacts.

ACKNOWLEDGMENTS

This work was performed at Sandia, which is a multiprogram laboratory operated by Sandia Corporation--a Lockheed Martin Company and at North Carolina State University. The work was supported by the United States Department of Energy under Contract DE-AC04-94AL85000. The authors also wish to acknowledge the instrumentation support provided by Digital Instruments, Santa Barbara CA.

REFERENCES

1. "Non-linear deformation mechanisms during nanoindentation," D.F. Bahr, D.E. Kramer, W.W. Gerberich, Acta Mater. **46**, 3605 (1998).

2. "Surface deformation of sapphire cystal," N.A. Nowak, Philo. Mag. A **74**, 171 (1996).

3. "Dislocation nucleation at nano-scale mechanical contacts," T.A. Michalske, J.E. Houston, Acta Materialia **46**, 391 (1998).

4. "Initial stages of yield in nanoindentation," J.D. Kiely, K.F. Jarausch, J.E. Houston, P.E. Russell, J. Mater. Res. **14**, 2219 (1999).

5. "Nanomechanical properties of Au (111), (001) and (110) surfaces," J.D. Kiely, J.E. Houston, Phys. Rev. B **57**, 12588 (1998).

6. "Effect of surface steps on the plastic threshold in nanoindentation," J.D. Kiely, R.Q. Hwang, J.E. Houston, Phys. Rev. Lett. **81**, 4424 (1998).

7. "Anomalous plastic deformation at surfaces: Nanoindentation of gold single cystals," S.G. Corcoran, R.J. Colton, E.T. Lilleodden, W.W. Gerberich, Phys. Rev. B **55**, R16057 (1997).

8. "Indentation induced dislocation nucleation: the initial yield point," W.W. Gerberich, J.C. Nelson, E.T. Lilleodden, P. Anderson, J.T. Wyrobek, Acta Mater. **44**, 3585 (1996).

9. "Dislocation distribution under a microindentation into a iron-silicon single crystal," W. Zielinski, H. Huang, S. Venkataraman, W.W. Gerberich, Philo. Mag. A **72**, 1221 (1995).

10. "Characterization of the induced plastic zone in a single crystal TiN(001) film by nanoindentation and transimission electron microscopy," M. Oden, H. Ljungcrantz, L. Hultman, J. Mater. Res. **12**, 2134 (1997).

11. "Microscopy and microindentation mechanics of single crystal Fe-3 wt. % Si: Part I: Atomic force microscopy of small indentation," S. Harvey, H. Huang, S. Venkataraman, W.W. Gerberich, J. Mater. Res. **8**, 1291 (1993).

12. "The injection of plasticity by millinewton contacts," W.W. Gerberich, S.K. Venkataraman, H. Huang, S.E. Harvey, D.L. Kohlstedt, Acta Metall. Mater. **43**, 1569 (1995).

13. "Microscopy and microindentation mechanics of single crystal Fe-3 wt. % Si: Part II: TEM of the indentation plastic zone," W. Zielinski, H. Huang, S. Venkataraman, W.W. Gerberich, J. Mater. Res. **8**, 1300 (1993).

14. "Nanoindentation of silver-relations between hardness and dislocation structure," G.M. Pharr, W.C. Oliver, J. Mater. Res. **4**, 94 (1989).

15. "Dislocation nucleation and defect structure during surface indentation," C.L. Kelchner, S.J. Plimpton, J.C. Hamilton, Phys. Rev. B **58**, 11085 (1998).

16. "Atomistic simulations of the nanometer-scale indentation of amorphous-carbon thin films," S.B. Sinnott, R.J. Colton, C.T. White, O.A. Shenderova, D.W. Brenner, J.A. Harrison, J. Vac. Sci. Technol. A **15**, 936 (1997).

17. "Nanomechanics and dynamics of tip-substrate interactions," U. Landman, W.D. Luedtke, J. Vac. Sci. Technol. B **9**, 414 (1991).

18. "Contact, nanoindentation, and sliding friction," A. Buldum, S. Ciraci, I.P. Batra, Phys. Rev. B **57**, 2468 (1998).

19. "Molecular dynmaics simulation of mechanical deformation of ultra-thin metal and ceramic films," J. Belak, J.N. Glosli, D.B. Boercker, I.F. Stowers, Mat. Res. Soc. Symp. Proc. **389**, 181 (1995).

20. "STM characterization of extended dislocation configurations in Au(001)," J. de la Figuera, M.A. Gonzalez, R. Garcia-Martinez, J.M. Rojo, O.S. Hernan, A.L. Vazquez de Paraga, R. Miranda, Phys. Rev. B **58**, 1169 (1998).

21. "A new force sensor incorporating force-feedback control for interfacial force microscopy," Joyce, S.A., Houston, J.E., Rev. Sci. Instrum. **62**, 710 (1991).

22. "The mechanical response of gold substrates passivated by self-assembling monolayer films," R.C. Thomas, J.E. Houston, T.A. Michalske, R.M. Crooks, Science **259**, 1883 (1993).

23. K.L. Johnson, *Contact Mechanics* (Cambridge University Press, Cambridge England 1996).

24. S.P. Timoshenko and J.N. Goodier, *Theory of Elasticity* (McGraw-Hill, New York 1970), 3rd ed.

25. "Chemically and Geometrically Enhanced Focused Ion Beam Micromachining," P.E. Russell, T.J. Stark, D.P. Griffis, J.R. Phillips, K.F. Jarausch, JVST B **16**, 2494 (1998).

27. TG101, NT-MDT, http://www.nt-mdt.com

28. "Size dependent hardness of silver crystals," Qing Ma, D.R. Clarke, J. Mater. Res. **10**, 853 (1995).

29. "A model for nano-indentation creep," W.B. Li, R. Warren, Acta Metall. Mater. **41**, 3065 (1993).

30. "Nanoindentation creep of single-crystal tungsten and gallium arsenide," Philo. Mag. A **76**, 1105 (1997).

26. JEOL 6400FE, JEOL, Boston MA.

FIGURE CAPTIONS

Figure 1. Images of the diamond indenters used in this study. The diamonds were prepared using a FIB micromachining process [25]. (a) is a SEM view of the three-sided indenter from 90 degrees to the indenter axis, (b) is a top down view and (c) is a 100 kx TEM micrograph illustrating its parabolic end-radius. (d) and (c) are SEM images of the parabolic indenter.

Figure 2. IFM load-displacement curve illustrating the elastic response of a Au (111) surface. The loading, unloading and Hertzian curves overlap, confirming the formation of an elastic contact between the indenter and the surface.

Figure 3. (a) Load-displacement curve illustrating the first stage of plasticity (stage I). This first stage of plasticity is characterized by slight deviations from the elastic (Hertzian) prediction.

(b) IFM image acquired before indentation, showing two surface steps (0.25 nm high) and two vacancy clusters (0.25 nm deep).

(c) IFM image acquired after indentation, showing a residual indentation that does not appear to reflect the crystallographic orientation of the surface and which is not associated with the formation of pileup.

(d) Cross-section view illustrating the imaged depth of the residual indentation, which closely matches the hysterisis of the load-displacement curve shown in (a).

Figure 4. Load-displacement curve illustrating stage II plasticity. Three stages of deformation are evident: elastic or Hertzian (dashed line), stage I plastic characterized by minor relaxations from the Hertzian prediction (between the solid and open arrow), and stage II plastic characterized by major relaxtions in the load-displacement curve (beginning at the open arrow).

Figure 5. IFM image acquired after indentation with a three-sided diamond indenter (the associated load-displacement curve is shown in Fig. 3). The pileup regions are visible as terraces, raised in 0.25 nm steps above the initial surface and bounded by (111) planes. Pileup formation is screened on the right indenter face by the presence of the previous indentation partially visible in the upper right of the image.

Figure 6. IFM image acquired after indentation with a parabolic diamond indenter. The residual indentation shows three-fold symmetry and the pileup regions form a six-fold rosette.

FIGURES

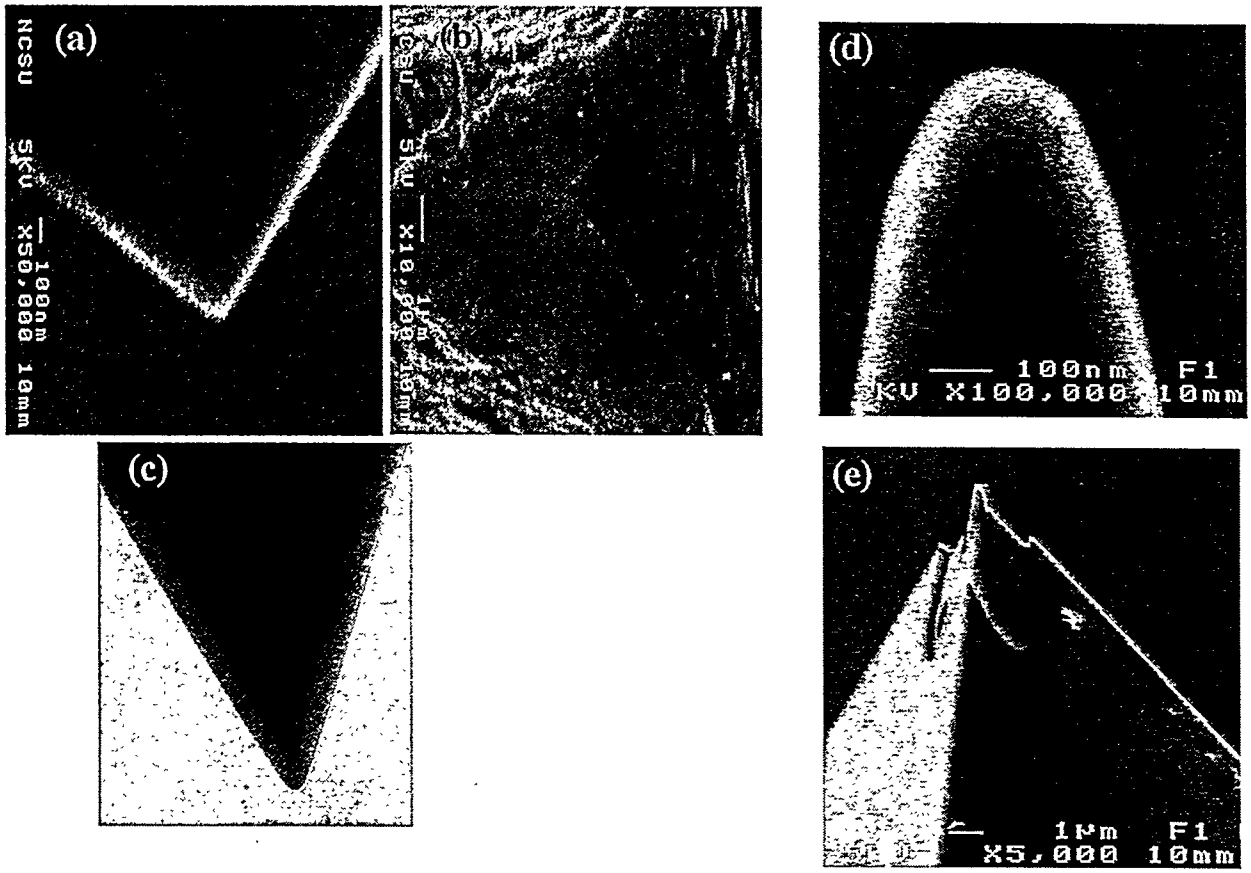

Figure 1.

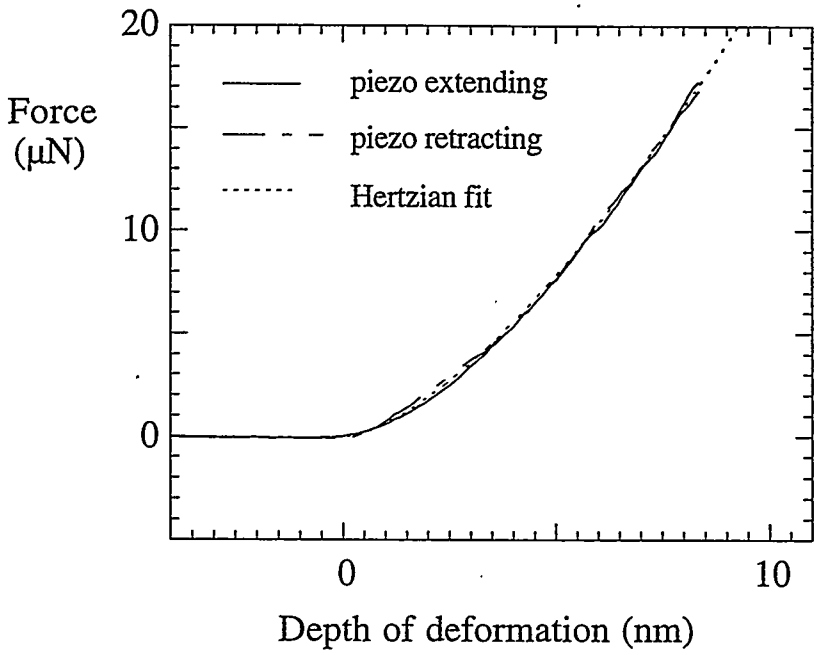
20
Force
(μN)
10
0
piezo extending
piezo retracting
Hertzian fit
0
10
Depth of deformation (nm)

Figure 2.

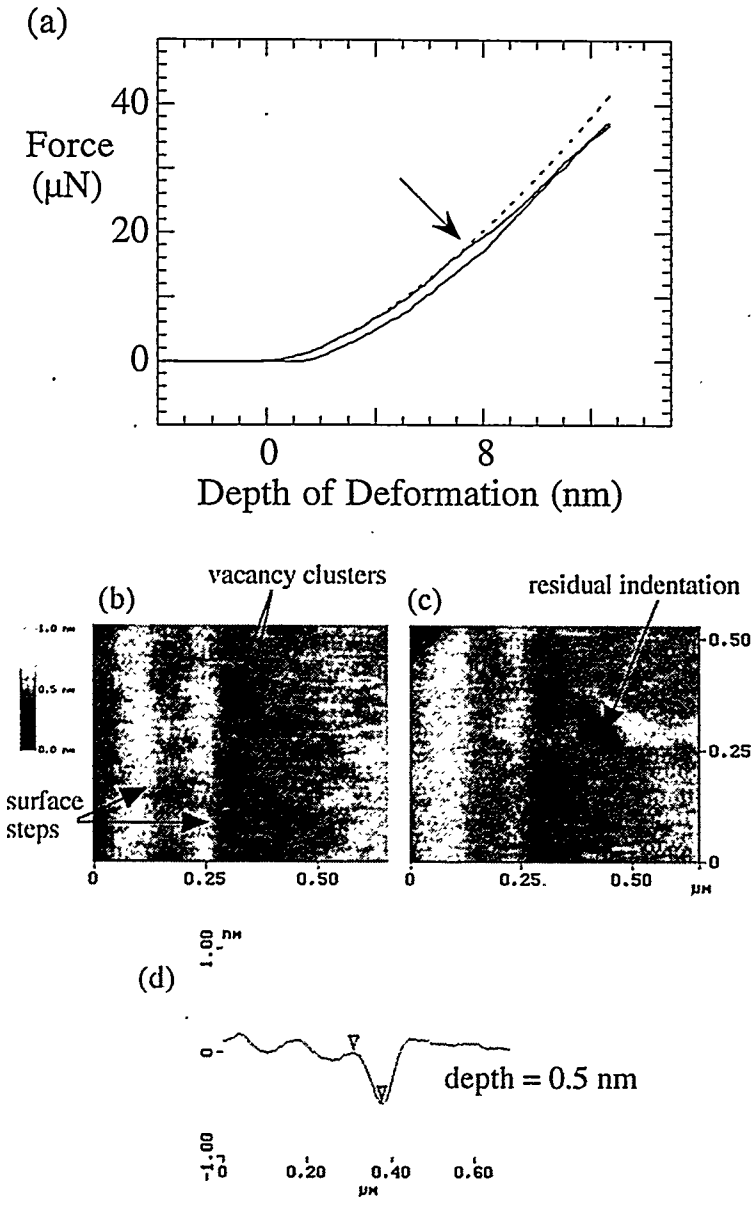
(a)
40
Force
(μN)
20
0
0
8
Depth of Deformation (nm)
(b)
vacancy clusters
(c)
residual indentation
surface
steps
0
0.25
0.50
0.50
0.25
0
μm
(d)
depth = 0.5 nm
0
0.20
0.40
0.60
μm

Figure 3.

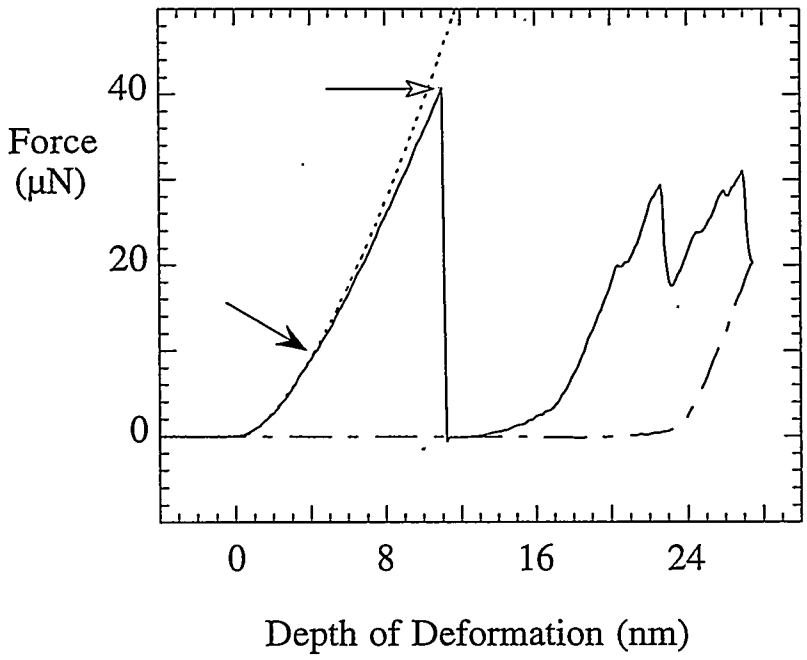

Figure 4.

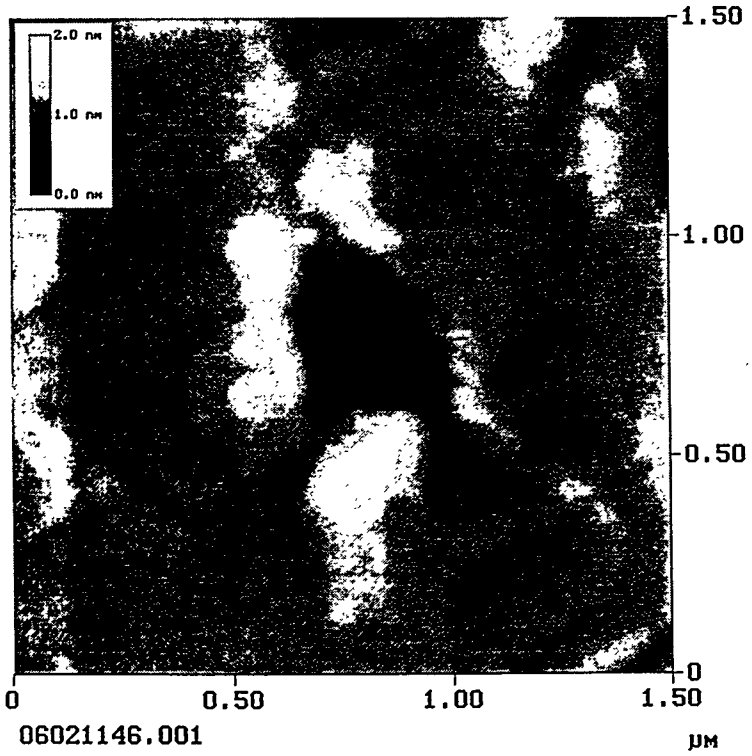

Figure 5.

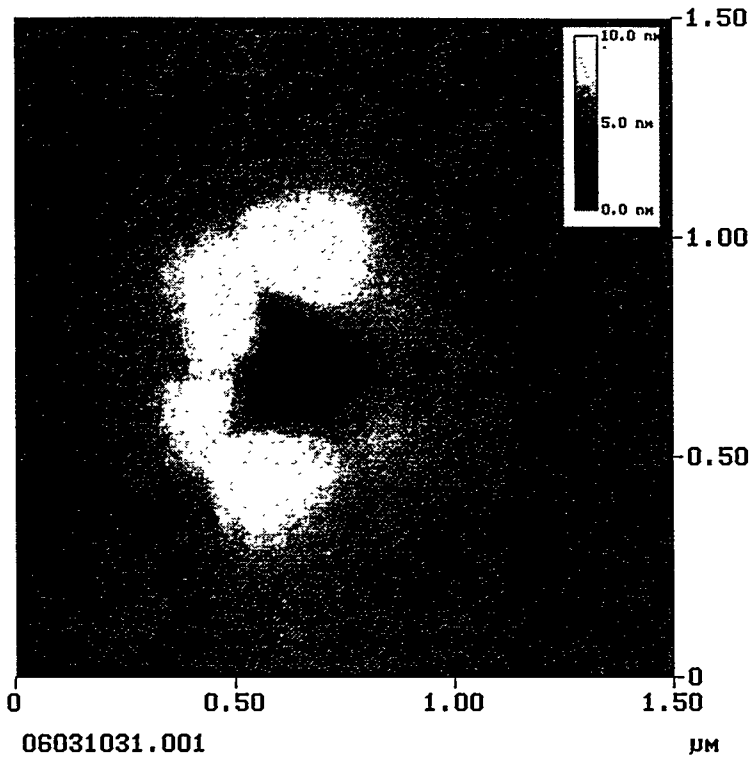

Figure 6.